

HEAVY FLAVOUR HIGHLIGHTS FROM THE LHCb*

ANDREA MAURI

on behalf of the LHCb Collaboration

Physik-Institut, University of Zurich
Winterthurerstrasse 190, 8057 Zurich, Switzerland*(Received April 14, 2017)*

This document presents an overview of the flavour anomalies observed by the LHCb experiment. All results are based on the dataset collected during the full LHC Run 1 by the LHCb Collaboration. Measurements of branching fractions of several $b \rightarrow sll$ decays are presented together with the angular analysis of $B^0 \rightarrow K^* \mu^+ \mu^-$ decays and the lepton flavour universality tests $R(K)$ and $R(D^*)$. In addition, a direct search for a new light scalar particle in the $B^+ \rightarrow K^+ \chi$ decay, with $\chi \rightarrow \mu^+ \mu^-$, is presented.

DOI:10.5506/APhysPolB.48.1073

1. Introduction

Even though the Standard Model (SM) provides solid predictions up to few hundreds GeV, it cannot explain all phenomena observed in the universe (dark matter, insufficient CP violation for the generation of a matter dominated universe, *etc.*). The present challenge is to find signals of new physics (NP) beyond the SM, but depending on the scale of NP, it might be that new particles are too heavy to be accessible through direct production. In this scenario, the only opportunity to detect NP would be looking for indirect effects from virtual particles in precisely predicted SM processes. The LHCb [1] experiment is a forward spectrometer dedicated to precision measurements of CP violation and rare decays of B hadrons at the LHC, and is an excellent environment for such precision tests of the SM.

All measurements presented here are based on the full LHC Run 1 data sample recorded by the LHCb experiment. The data consists of proton–proton collisions at centre-of-mass energies of 7 and 8 TeV, and corresponds to an integrated luminosity of 3.0 fb^{-1} .

* Presented at the Cracow Epiphany Conference “Particle Theory Meets the First Data from LHC Run 2”, Kraków, Poland, January 9–12, 2017.

2. $b \rightarrow sll$ transitions: branching fractions measurements

Processes involving $b \rightarrow sll$ flavour-changing neutral current (FCNC) transition are powerful probes of NP. In the SM, FCNC decays can only proceed via loop diagrams (“penguin” or box diagram, as shown in Fig. 1), which are suppressed and hence more sensitive to NP. New heavy particles can appear, potentially both at tree and loop level, and significantly change the branching fraction of these processes, as well as the angular distributions of the final-state particles.

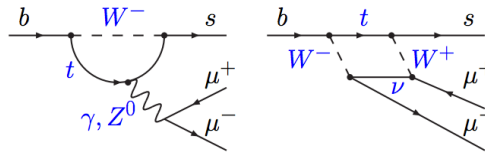


Fig. 1. Loop diagrams of $b \rightarrow sll$ transitions.

Figure 2 shows the measurement of the branching fractions of several channels: $B^+ \rightarrow K^+ \mu^+ \mu^-$, $B^0 \rightarrow K^0 \mu^+ \mu^-$, $B^+ \rightarrow K^{*+} \mu^+ \mu^-$ [2], $B_s^0 \rightarrow \phi \mu^+ \mu^-$ [3] and $\Lambda_b \rightarrow \Lambda \mu^+ \mu^-$ [4]. The measured branching fractions are found to be consistently lower than the SM prediction, especially in the low-central region of q^2 , the invariant mass squared of the dimuon system.

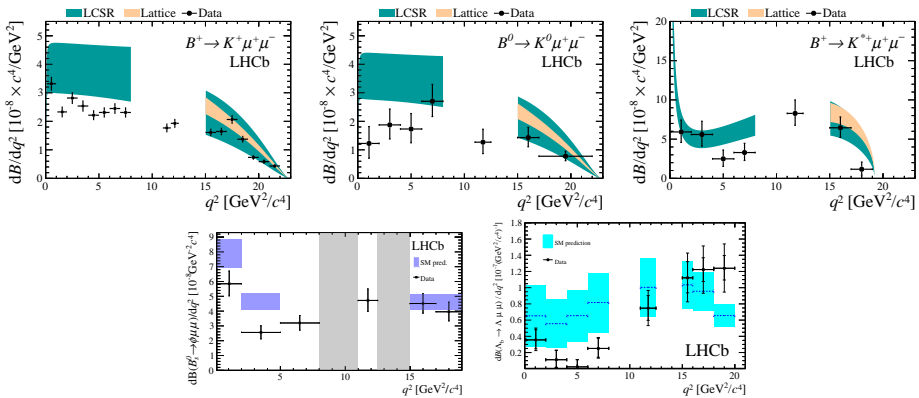


Fig. 2. Differential branching fractions measurements overlaid with SM predictions for: (top) $B^+ \rightarrow K^+ \mu^+ \mu^-$, $B^0 \rightarrow K^0 \mu^+ \mu^-$ and $B^+ \rightarrow K^{*+} \mu^+ \mu^-$ decays [2]; (bottom) $B_s^0 \rightarrow \phi \mu^+ \mu^-$ [3] and $\Lambda_b \rightarrow \Lambda \mu^+ \mu^-$ [4] decays.

3. Angular analysis of $B^0 \rightarrow K^* \mu^+ \mu^-$ decay

Due to the presence of a vector meson in the final state, the $B^0 \rightarrow K^{*0} \mu^+ \mu^-$ decay provides a richer phenomenology than the simple branching fraction measurement. Its final state can be described by q^2 and three

decay angles (θ_l , θ_k and ϕ). A clean set of angular-observables with reduced form-factor uncertainties was proposed in Ref. [5]. While most of the angular observables are found to be compatible with the SM predictions, a discrepancy is observed in P'_5 in two bins of q^2 (Fig. 3) [6]. This deviation was later confirmed by the Belle experiment [7].

Literature is rich of possible interpretations trying to explain this deviation, appealing to unexpectedly large hadronic effects (*charm-loop effect*) [8, 9] or invoking NP [10, 11]. In the latter scenario, a global fit to the $B^0 \rightarrow K^{*0} \mu^+ \mu^-$ angular analysis and several $b \rightarrow sll$ and $b \rightarrow sll\gamma$ branching fraction measurements results in a deviation of 3.7σ from the SM, where only the C_9 Wilson coefficient is allowed to float [10]. Figure 3 also shows the result of the fit in the C_9 – C_{10} plane.

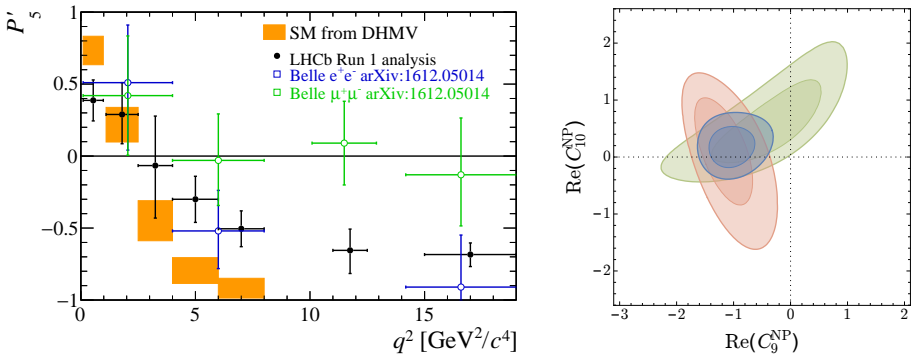


Fig. 3. (Colour on-line) Left: The optimised angular observable P'_5 in bins of q^2 , determined from a maximum likelihood fit to the data. The LHCb measurement is shown overlaid with the Belle result [7]. The shaded boxes show the SM prediction taken from Ref. [12]. Right: Allowed regions in the $\text{Re}(C_9^{\text{NP}})$ – $\text{Re}(C_{10}^{\text{NP}})$ plane [10], the dark grey/blue contours correspond to the 1 and 2σ best fit regions from the global fit, the light grey/green and grey/red contours correspond to the 1 and 2σ regions if only branching fraction data or only data on $B^0 \rightarrow K^* \mu^+ \mu^-$ angular observables is taken into account.

4. Lepton universality test: $R(K)$ measurement

Additional tests of the SM performed with $b \rightarrow sll$ decays concern lepton flavour universality (LFU). Once the difference of the lepton mass has been taken into account, amplitudes of processes involving different lepton flavours should be identical in the SM. To cancel out most of the experimental uncertainties related to the hadronic part of the decay, it is common to define the ratio $R(K)$ as the ratio of branching fractions of the $B^+ \rightarrow K^+ \mu^+ \mu^-$ decay with respect to the $B^+ \rightarrow K^+ e^+ e^-$ decay. $R(K)$ is predicted to be unity with a very good accuracy in the SM [13]. The

measured value of $R(K)$ is $0.745^{+0.090}_{-0.074} \pm 0.036$ [14] and shows a deviation with respect to the SM prediction at the level of 2.6σ (see Fig. 4). In some NP scenario, this tension can be interpreted in a coherent way with the $B^0 \rightarrow K^*\mu^+\mu^-$ anomaly and, moreover, eventual violation of LFU cannot be explained by the charm-loop effect.

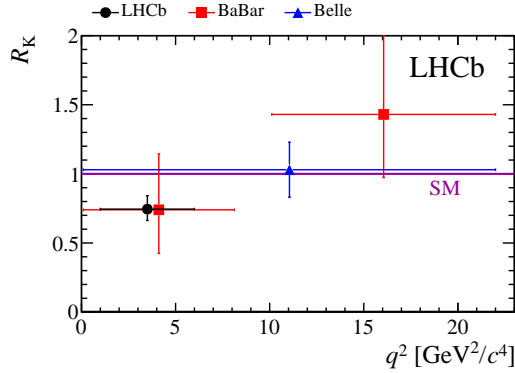


Fig. 4. $R(K)$ measurement from the LHCb [14], Babar [15] and Belle [16] experiments.

5. Lepton universality test: $R(D^*)$ measurement

Similar LFU tests can be performed exploiting other decay modes, like $B \rightarrow D^*l\nu$. In this case, one can define the ratio $R(D^*)$ as the ratio of branching fractions of the $B^0 \rightarrow D^{*+}\tau^-\bar{\nu}_\tau$ decay to the $B^0 \rightarrow D^{*+}\mu^-\bar{\nu}_\mu$ decay. For this measurement, the D^{*+} meson is reconstructed in the $D^0(K^-\pi^+)\pi^+$ final state, while the charged τ lepton is reconstructed in its purely leptonic mode $\tau \rightarrow \mu\bar{\nu}_\mu\nu_\tau$. Two main experimental challenges follow this choice. Firstly, the two decay modes share the same visible final state, and secondly, one and three neutrinos are respectively present in the two considered final states, carrying out missing energy and smearing the reconstructed mass distributions. Figure 5 shows the separation of the tauonic and muonic yields together with the backgrounds distribution in two variables with high discriminating power, the missing mass squared, m_{miss}^2 , and the muon energy E_μ .

Figure 6 shows the measured value of $R(D^*) = 0.336 \pm 0.027 \pm 0.030$ [17] and confirms the tension already seen at B -factories [18] with respect to the SM prediction of $R(D^*) = 0.252 \pm 0.003$ [19], where $R(D^*)$ differs from unity because of the difference in phase space due to the $\tau - \mu$ mass difference. The world average of the $R(D^*)$ and $R(D)$ measurements reports a 3.9σ deviation from the SM [20] creating an interesting pattern with the anomaly in the $R(K)$ measurement. Models of NP that couple differently to the three generations of leptons could, in fact, coherently explain the observed deviations [21].

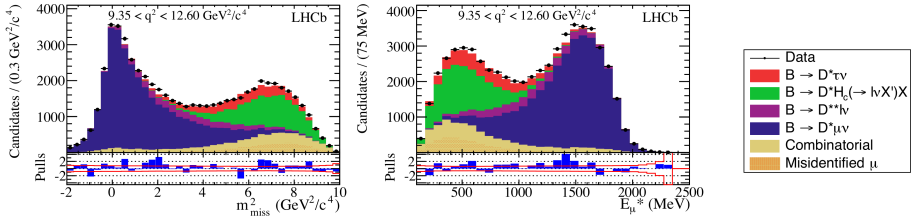


Fig. 5. Projection of the fit model in one of the four q^2 bins. Binned m_{miss}^2 , E_μ and q^2 distributions are fitted using a three-dimensional template (signal from MC and backgrounds from data).

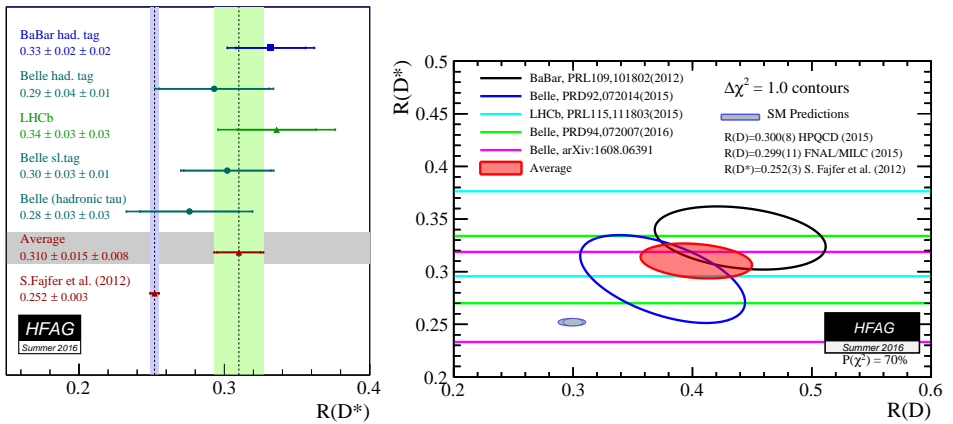


Fig. 6. Single $R(D^*)$ and combined with $R(D)$ measurements from different experiments compared to SM predictions [20].

6. Search for long-lived scalar particles in $B^+ \rightarrow K^+ \chi(\mu^+ \mu^-)$ decays

Rare B decays occurring through FCNC can also be a valid framework for direct searches of NP. Many models predict the existence of a Hidden Sector of particles that can only communicate with the SM via a weakly interacting mediator. In the Higgs portal scenario, a hypothetical new scalar particle, χ , namely the inflaton (associated to the field that generates the inflation of the early Universe), can mix with the SM Higgs boson and, if it is light, can be produced in B decays [22–24].

A search for a new scalar particle is performed studying the $B^+ \rightarrow K^+\chi$ decay, with $\chi \rightarrow \mu^+\mu^-$, as illustrated in Fig. 7. The dimuon vertex is allowed, but not required, to be displaced from the B -decay vertex. The inflaton mass and lifetime are theoretically weakly constrained; current experimental limits are set by the CHARM experiment [25] and a previous search at the LHCb [26].

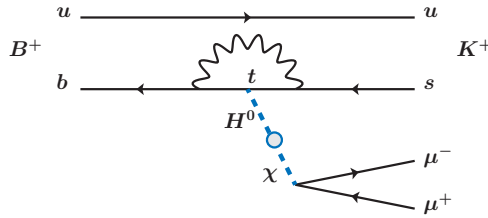


Fig. 7. Feynman diagram for the $B^+ \rightarrow K^+\chi$ decay, with $\chi \rightarrow \mu^+\mu^-$.

The strategy of the search consists in scanning the kinematically allowed dimuon mass range, looking for a new dimuon resonance on top of the SM $B^+ \rightarrow K^+\mu^+\mu^-$ decays [27]. Obviously, the well-known SM resonances ϕ , J/ψ , $\psi(2S)$, $\psi(3770)$ and $\psi(4160)$ must be vetoed from the search. The sensitivity is enhanced by considering three regions of the dimuon decay time $t(\mu^+\mu^-)$: a prompt, an intermediate and an extremely displaced region. This division follows the very different background yields expected in the three regions; the main $B^+ \rightarrow K^+\mu^+\mu^-$ SM background, in fact, is characterized by prompt dimuon vertex and the first decay-time region is defined as $|t(\mu^+\mu^-)| < 1$ ps, in order to contain all this irreducible source of background. The residual background that can populate the displaced regions of the analysis consists of combinatorial background. The division between the second and third decay-time region is chosen such to expect less than one background event in the full dimuon mass range of the third region. To reduce the level of combinatorial background, a multivariate selection is applied and each decay-time region of the analysis is optimized separately.

Figure 8 shows the mass distribution of the observed number of events in the first and second decay-time regions, while no events are observed in the third region. For each value of $m(\chi)$ and $\tau(\chi)$, the background plus signal and the background-only hypotheses are compared using the C.L.s method, where the information from the three decay-time regions are combined. For each tested mass, the expected number of background events is obtained by a linear interpolation of the dimuon mass sidebands, while the shape of the signal mass distribution is taken from simulation. No significant signal excess compared to the background-only hypothesis is found, thus upper limits on the branching fraction of the decay $B^+ \rightarrow K^+\chi(\mu^+\mu^-)$ are set as a function of the inflaton mass and lifetime as shown in Fig. 9. The

upper limits vary between 2×10^{-10} and 10^{-7} , and are most stringent in the region around $\tau(\chi) = 10$ ps. Lower lifetimes suffer the large background contamination, while for longer lifetime, the fraction of signal candidates that escape from the detector acceptance becomes dominant.

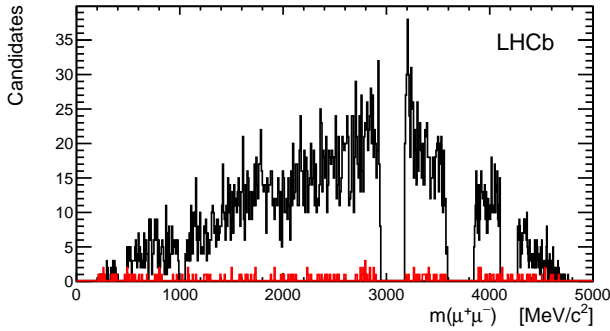


Fig. 8. (Colour on-line) Distribution of the $m(\mu^+\mu^-)$ in the first (black) and second (grey/red) decay-time region of the search.

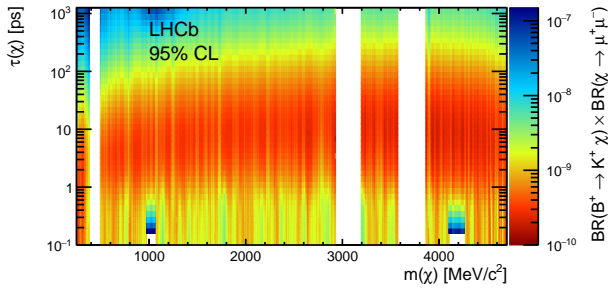


Fig. 9. Excluded branching fraction for the $B^+ \rightarrow K^+\chi(\mu^+\mu^-)$ decay as a function of $m(\chi)$ and $\tau(\chi)$ at 95% C.L.

Figure 10 presents the interpretation of the result in term of the inflaton model introduced in Refs. [22–24]. Constraints are placed on the parameter space given by the mass and the square of the mixing angle, θ^2 , of the inflaton with the Higgs boson, which appears in the effective coupling of the inflaton to the SM particles.

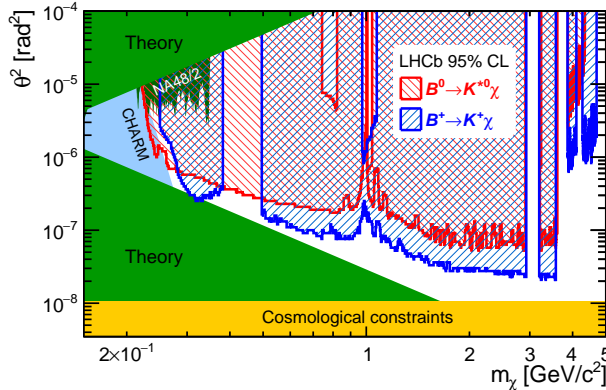


Fig. 10. (Colour on-line) Parameter space of the inflaton model described in Refs. [22–24]. The region excluded at 95% C.L. by this analysis is shown by the black/blue hatched area. The region excluded by the search with the $B^0 \rightarrow K^{*0} \chi(\mu^+ \mu^-)$ decay [26] is indicated by the grey/red hatched area. Direct experimental constraints set by the CHARM experiment [25] and regions forbidden by theory or cosmological constraints [24] are also shown.

7. Conclusion

Flavour physics is an extremely promising sector for the search of NP. In the recent years, some tensions with respect to the SM appeared in FCNC processes involving $b \rightarrow sll$ transitions as well as in the LFU measurement $R(K)$ and $R(D^*)$. Discrepancies were observed not only by the LHCb experiment but also at the B -factories. The anomalies may fit in a coherent pattern of NP involving the C_9 and C_{10} Wilson coefficients.

Since most of these results are dominated by the statistical uncertainty, it will be fundamental to publish updates including the additional data taken during the LHC Run 2. Additional measurements are also of extreme importance, for example the angular analysis of $B \rightarrow K^* e^+ e^-$ or the study of more LFU related processes like $R(K^*)$ and $R(\phi)$ or the semitauonic $R(D^+)$ or $R(D^*)$ with a fully hadronic τ reconstruction.

A direct search for new particles at the LHCb has also been presented which provides the best experimental constraints to date on light inflaton models.

REFERENCES

- [1] A.A. Alves, Jr. *et al.* [LHCb Collaboration], *JINST* **3**, S08005 (2008).
- [2] R. Aaij *et al.* [LHCb Collaboration], *J. High Energy Phys.* **1406**, 133 (2014) [arXiv:1403.8044 [hep-ex]].
- [3] R. Aaij *et al.* [LHCb Collaboration], *J. High Energy Phys.* **1509**, 179 (2015) [arXiv:1506.08777 [hep-ex]].

- [4] R. Aaij *et al.* [LHCb Collaboration], *J. High Energy Phys.* **1506**, 115 (2015) [arXiv:1503.07138 [hep-ex]].
- [5] S. Descotes-Genon, T. Hurth, J. Matias, J. Virto, *J. High Energy Phys.* **1305**, 137 (2013) [arXiv:1303.5794 [hep-ph]].
- [6] R. Aaij *et al.* [LHCb Collaboration], *J. High Energy Phys.* **1602**, 104 (2016) [arXiv:1512.04442 [hep-ex]].
- [7] S. Wehle *et al.* [Belle Collaboration], *Phys. Rev. Lett.* **118**, 111801 (2017) [arXiv:1612.05014 [hep-ex]].
- [8] J. Lyon, R. Zwicky, arXiv:1406.0566 [hep-ph].
- [9] M. Ciuchini *et al.*, *J. High Energy Phys.* **1606**, 116 (2016) [arXiv:1512.07157 [hep-ph]].
- [10] W. Altmannshofer, D.M. Straub, arXiv:1503.06199 [hep-ph].
- [11] S. Descotes-Genon, L. Hofer, J. Matias, J. Virto, *J. High Energy Phys.* **1606**, 092 (2016) [arXiv:1510.04239 [hep-ph]].
- [12] S. Descotes-Genon, L. Hofer, J. Matias, J. Virto, *J. High Energy Phys.* **1412**, 125 (2014) [arXiv:1407.8526 [hep-ph]].
- [13] C. Bouchard *et al.* [HPQCD Collaboration], *Phys. Rev. Lett.* **111**, 162002 (2013) [Erratum *ibid.* **112**, 149902 (2014)] [arXiv:1306.0434 [hep-ph]].
- [14] R. Aaij *et al.* [LHCb Collaboration], *Phys. Rev. Lett.* **113**, 151601 (2014) [arXiv:1406.6482 [hep-ex]].
- [15] J.P. Lees *et al.* [BaBar Collaboration], *Phys. Rev. D* **86**, 032012 (2012) [arXiv:1204.3933 [hep-ex]].
- [16] J.-T. Wei *et al.* [Belle Collaboration], *Phys. Rev. Lett.* **103**, 171801 (2009) [arXiv:0904.0770 [hep-ex]].
- [17] R. Aaij *et al.* [LHCb Collaboration], *Phys. Rev. Lett.* **115**, 111803 (2015) [Addendum *ibid.* **115**, 159901 (2015)] [arXiv:1506.08614 [hep-ex]].
- [18] J.P. Lees *et al.* [BaBar Collaboration], *Phys. Rev. Lett.* **109**, 101802 (2012) [arXiv:1205.5442 [hep-ex]].
- [19] S. Fajfer, J.F. Kamenik, I. Nisandzic, *Phys. Rev. D* **85**, 094025 (2012) [arXiv:1203.2654 [hep-ph]].
- [20] Y. Amhis *et al.*, arXiv:1612.07233 [hep-ex].
- [21] M. Bauer, M. Neubert, *Phys. Rev. Lett.* **116**, 141802 (2016) [arXiv:1511.01900 [hep-ph]].
- [22] B. Batell, M. Pospelov, A. Ritz, *Phys. Rev. D* **83**, 054005 (2011) [arXiv:0911.4938 [hep-ph]].
- [23] F. Bezrukov, D. Gorbunov, *J. High Energy Phys.* **1005**, 010 (2010) [arXiv:0912.0390 [hep-ph]].
- [24] F. Bezrukov, D. Gorbunov, *J. High Energy Phys.* **1307**, 140 (2013) [arXiv:1303.4395 [hep-ph]].
- [25] F. Bergsma *et al.* [CHARM Collaboration], *Phys. Lett. B* **157**, 458 (1985).
- [26] R. Aaij *et al.* [LHCb Collaboration], *Phys. Rev. Lett.* **115**, 161802 (2015) [arXiv:1508.04094 [hep-ex]].
- [27] M. Williams, *JINST* **10**, P06002 (2015) [arXiv:1503.04767 [hep-ex]].